Journal of
Nanoscience and Nanotechnology
Vol. 12, 5816–5819, 2012

RESEARCH ARTICLE

Infrared Conductivity and Carrier Mobility of Large Scale Graphene on Various Substrates

Joo Youn Kim[1], Jae Hoon Rho[1], Chul Lee[1], Sukang Bae[3], Sang Jin Kim[3], Keun Soo Kim[4], Byung Hee Hong[2], and E. J. Choi[1,*]

[1] Department of Physics, University of Seoul, Seoul 130-743, Republic of Korea
[2] Department of Chemistry, Seoul National University, Seoul 151-742, Republic of Korea
[3] SKKU Advanced Institute of Nanotechnology, Sung Kyun Kwan University, Suwon 440-746, Republic of Korea
[4] Department of Physics and Graphene Research Institute, Sejong University, Seoul 143-747, Republic of Korea

It is known that low-field mobility of graphene depends largely on the substrate material on which it is transferred. We measured Drude optical conductivity of graphene on various substrates and determined the carrier density and carrier scattering rate. The carrier density varies widely depending on the substrate material. However the scattering rate is almost constant, ~100 cm^{-1}, for 5 different substrates. We calculate carrier mobility of graphene using the two quantities, i.e., carrier density and scattering rate, to find that it agrees with the mobility measured from dc transport experiment. We conclude that substrate-depent mobility of graphene originates from different carrier density but not from the scattering rate.

Keywords: CVD Graphene, Substrate Effect, Infrared FTIR.

1. INTRODUCTION

To enhance carrier mobility of graphene is an important task in high-speed electronic device application. For suspended or free standing graphene carrier mobility can be as high as $\mu = 250{,}000\ cm^2/V \cdot s$ at room temperature.[1] When it is transferred on SiO_2/Si substrate, however, μ is reduced largely to 3,000~15,000 $cm^2/V \cdot s$.[2] When graphene is transferred on substrate carrier density (N) changes due to substrate-induced charge doping. Also the scattering rate (Γ) is believed to increase due to various scattering centers such as surface polar phonon and charged impurity of the substrate. N and Γ are, as we will discuss later, directly related with the carrier mobility of graphene. At this point it is believed widely that the reduction of mobility of graphene on substrate is due to latter effect, i.e., increased carrier scattering, however, without detailed experimental support.

To understand the fundamental problem of grapheme mobility of how it changes on differnt substrate it is that important to characterize N and Γ for various types of substrate materials. N and Γ are measured commonly by Hall effect and dc-resistivity experiment. Recently we and other groups reported[3,4] that they can be determined from Far-infrared spectroscopy of free carrier Drude response. This method allows simultaneous measurement of N and Γ without need of the electrical-lead contact to the sample.

In this work we performed Far-IR (FIR) transmission measurement of large scale Chemical Vapor Deposition (CVD)-grown graphene placed on b-layer/SiO_2 composite substrate. Here b-layers represent bufferlayer we deposited on top of SiO_2. We have prepared two groups of b-layer: (1) polar dielectric oxide ($SrTiO_3$ and ZnO) and (2) organic polymer film HMDS ($[(CH_3)_3Si]_2NH$) and polymethyl methacrylate (PMMA; $(C_5O_2H_8)_n$). We also measured the sample with no b-layer, graphene/SiO_2. From FIR transmission measurement we determine optical conductivity of large scale graphene and extract N and Γ for different substrates. It allows us to understand the origin of mobility change on substrate, which is important for application of large scale graphene (LSG) as photovoltaic device,[5,6] flexible display,[7] and transparent conductor.[8]

2. EXPERIMENTAL DETAILS

LSG is synthesized by CVD method as described elsewhere.[9] b-layer was despoited on SiO_2 (300 nm thick)/Si-substrate using thermal evaporation method as in

*Author to whom correspondence should be addressed.

1533-4880/2012/12/5816/004 doi:10.1166/jnn.2012.6347

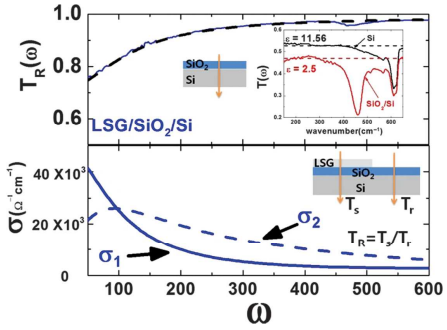

Fig. 1. $T_R(\omega)$ (upper panel) and optical conductivity (lower panel) of graphene transferred on SiO_2 (300 nm)/Si (0.5 mm) substrate measured in Far-IR region. $T_R(\omega)$ represents the transmission relative to that of the substrate. The dashed curve shows the Drude model fit result. The inset shows absolute transmission of SiO_2 (300 nm)/Si (0.5 mm) and Si (0.5 mm) without graphene. The dip at 460 cm^{-1} (610 cm^{-1}) is due to optical phonon of SiO_2(Si). σ_1 and σ_2 are the real and imaginary part of the optical conductivity $\sigma(\omega)$.

Refs. [10 and 12] (for $SrTiO_3$ and ZnO) and spin-coating method (HMDS and PMMA) respectively. Thickness of the b-layer was measured using AFM and ellipsometry method. LSG was transferred onto the composite substrate b-layer/SiO_2/Si after removing Cu-foil using 0.1 M ammonium persulphate $(NH_4)_2S_2O_8$ solution. For Far-IR measurement we covered half of the substrate surface with LSG leaving the other half for the transmission reference (see inset of Figs. 1 and 2). Transmission spectrum through LSG/sub ($=T_s$) was normalized by that through the bare substrate ($=T_r$) and relative transmission $T_R(\omega) = T_s/T_r$ was obtained. FTIR (Bomem DA8) and bolometric detector were used for FIR measurement.

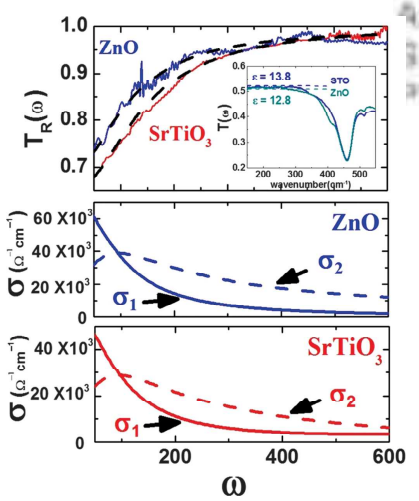

Fig. 2. (Top panel) $T_R(\omega)$ of graphene transferred on ZnO/SiO_2/Si and STO/SiO_2/Si. The dashed curves are the fitting results from the Drude model analysis. The inset shows absolute transmission of the bare substrates. (Middle and bottom panel) optical conductivity of graphene extracted from the fit.

3. RESULTS AND DISCUSSION

Figure 1 shows $T_R(\omega)$ in the Far infrared region measured on LSG/SiO_2 (300 nm)/Si. The curve rises at low frequency (=decrease of transmission) due to Drude absorption. The transmission of the SiO_2/Si substrate is flat with frequency without the phonon peak of SiO_2 (460 cm^{-1}) and Si (610 cm^{-1}) in inset, a typical behavior of an insulator. We fit $T_R(\omega)$ using three-layer model with dielectric function $\epsilon(\omega)$ algorithm:[11] $[\epsilon(\omega), d] = [11.6, 0.5$ mm$]$ for Si and $[2.5,$ 300 nm$]$ for SiO_2. d is the layer thickness. $\epsilon(\omega)$ was determined from transmission data in the inset. For LSG we use,[4] $[-(4\pi/i\omega)\sigma(\omega), 3.4$ Å$]$ where $\sigma(\omega)$ is the Drude optical conductivity

$$\sigma(\omega) = \frac{\omega_P^2}{4\pi} \cdot \frac{i}{\omega + i\Gamma} \tag{1}$$

Here Drude strength ω_P^2 and carrier scattering rate Γ are the fitting parameters. Interference among the multiply reflected lights is accounted for coherently for LSG and SiO_2 layers. The fit agrees well with the data. The lower panel shows the Drude optical conductivity of graphene obtained from the fit. Here σ_1 and σ_2 are the real and imaginary part of the optical conductivity $\sigma(\omega)$. The $2d$-carrier density N is related with ω_P as $\omega_P^2 \cdot d = (V_F e^2/\hbar)\sqrt{\pi N}$. Using the Fermi velocity $V_F = 1.1 \times 10^6$ m/s, we obtain $N = 4.5 \times 10^{12}$ cm^{-2} which is comparable to transport measurements.[12] We repeated the $T_R(\omega)$ measurement for six LSG samples and the data were reproduced with identical ω_P^2 and Γ values.

Figure 2 displays $T_R(\omega)$ of LSG on ZnO and $SrTrO_3$ layers. The Drude peak for ZnO-buffer is stronger than that for the SiO_2 layer of Figure 1, while it is similar for STO. From 4-layer model fit, we obtain $N = 9.8 \times 10^{12}$ cm^{-2} and $N = 5.6 \times 10^{12}$ cm^{-2} for ZnO and STO respectively. $\Gamma = 95\sim100$ cm^{-1} is the same as that of Figure 1.

Figure 3 plots $T_R(\omega)$ of LSG on organic films PMMA and HMDS. In PMMA Drude strength is substantially enhanced resulting in the increase of N to 11.8×10^{12} cm^{-2}. For HMDS, N is suppressed largely to $N = 0.1 \times 10^{12}$ cm^{-2}, which is 1/40 of that for SiO_2. In contrast to the N-change Γ is almost the same as for the other b-layers. Again the transmission of the bare HMDS.

(PMMA)/SiO_2/Si, inset of Figure 2, shows the insulating behavior of the buffer layers. The fitting parameters for the graphene layer and for the b-layers are summarized in Table I.

For the five samples we have studied in this work, Γ lies in $95\sim120$ cm^{-1} range. The little dependence of Γ on the b-layer is an unexpected result: In polar oxide substrate remote surface polar phonon (SPP) is considered as important scattering source for graphene at room-T.[13, 14] On the other hand HMDS is a non-polar material where SPP is absent or, if any, weak. Γ shows no difference for the two material groups. Charged impurity in the substrate

RESEARCH ARTICLE

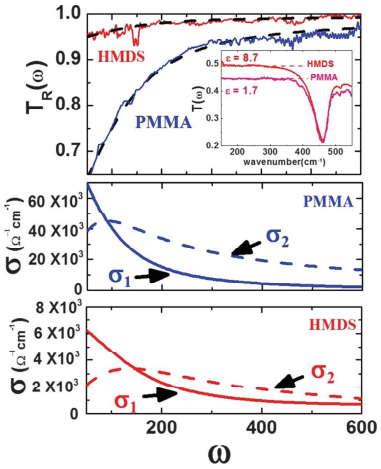

Fig. 3. $T_R(\omega)$ and optical conductivity of graphene on PMMA/SiO_2/Si and HMDS/SiO_2/Si.

is another scattering source for the carrier in graphene. In high-ϵ substrate, the Coulomb potential is screened more effectively by the dielectric polarization of the lattice. However while ϵ of the b-layer varies from 2.5 (for SiO_2) to 11 (for STO) in our measurement, Γ remains constant showing no correlation with ϵ (inset of Fig. 3).[15] The robustness of Γ may indicate that Γ is dominated by intrinsic scattering due to such as phonon of the graphene itself, the nano-ripples, and the grain boundary.

In graphene carrier mobility μ is given as $\mu = e/\sqrt{\pi}h \cdot ((V_F/\sqrt{N})1/\Gamma)$ in contrast with the familiar semiclassical relation $\mu = e/m \cdot 1/T$.[13] Using N and Γ of Table I we calculate μ for each b-layer (Table I). For LSG on SiO_2 we have $\mu \simeq 2500$ cm^2/V $\cdot$ s which is close to other reports.[16] Notably μ increases to 11,700 cm^2/V $\cdot$ s for HMDS. The significant μ-enhancement is due to the exceptionally small N of HMDS but not by reduced scattering rate. In fact Γ of HMDS is larger than other b-layers. To find a b-layer material with small N is one guideline toward better μ. However when LSG is applied as a field effect device N can increase by the gate voltage and in such situation μ-drop can not be avoided. Ultimately μ-increase through the reduced Γ is highly needed. Next step of our work is to find a way to improve Γ such as, for example, thermal annealing.

Table I. Drude model fit result for different buffer-layers: plasma frequency ω_P, scattering rate Γ, carrier density N, and mobility μ. d and ϵ are the thickness and dielectric constant respectively.

Type	d (nm)	ϵ	ω_p ($\times 10^3$ cm^{-1})	Γ cm^{-1}	N ($\times 10^{12}$ cm^{-2})	μ (cm^2/V $\cdot$ s)
SiO_2	300	2.5	17.4	95.0	4.5	2467
ZnO	30	12.8	21.1	100.0	9.8	1594
$SrTiO_3$	30	13.8	18.3	95.0	5.6	2216
HMDS	2	8.7	7.1	120.0	0.1	11680
PMMA	30	1.7	22.1	95.0	11.8	1527

4. CONCLUSIONS

In conclusion we have performed Far-IR spectroscopy measurement to investigate the effect of buffer-layer on graphene in the LSG/buffer-layer/SiO_2 (300 nm)/Si samples. The Drude response of graphene showed that (1) carrier density N changes depending on the five b-layers, polar oxide thin layer ZnO and $SrTiO_3$, organic film PMMA and HMDS, and the bare SiO_2. (2) However surprisingly the carrier scattering rate Γ has little dependence on the buffer-layers. That the carrier mobility μ varies on different substrates—including the fourfold enhancement to 11,700 (cm^2/V $\cdot$ s) for HMDS-layer—results through the N-change, but not from the Γ change as many people believe. Our finding indicates that in addition to the N-control further room is left open for μ-enhancement through Γ improvement.

Acknowledgments: This work research was supported by Basic Science Research Program through the NRF funded by the Ministry of Education, Science and Technology (Grant Nos. 2010-0008281, 2011-09012012 and 2011-0029645 for EJC, KSK and Grant Nos. 2011-0021972 and 2011-0017587 For BHH). JYK was supported by Hi Seoul Science Fellowship funded by Seoul Scholarship Foundation.

References and Notes

1. M. Orlita, C. Faugeras, P. Plochocka, P. Neugebauer, G. Martinez, D. K. Maude, A.-L. Barra, M. Sprinkle, C. Berger, and W. A. de Heer, *Phys. Rev. Lett.* 101, 267601 (**2008**).
2. S. V. Morozov, K. S. Novoselov, M. I. Katsnelson, F. Schedin, L. A. Ponomarenko, D. Jiang, and A. K. Geim, *Phys. Rev. Lett.* 97, 016801 (**2006**).
3. C. Lee, J. Y. Kim, S. K. Bae, K. S. Kim, B. H. Hong, and E. J. Choi, *Appl. Phys. Lett.* 98, 071905 (**2011**).
4. J. Horng, C. F. Chen, B. Geng, C. Girit, Y. Zhang, Z. Hao, H. A. Bechtel, M. Michael, A. Zettl, M. F. Crommie, Y. R. Shen, and F. Wang, *Phys. Rev. B* 83, 165113 (**2011**).
5. J. Wang, Y. Wang, D. He, H. Wu, H. Wang, P. Zhou, M. Fu, Ke Jiang, and W. Chen, *J. Nanosci. Nanotechnol.* 11, 9432 (**2011**).
6. H. Wang, D. He, Y. Wang, Z. Liu, H. Wu, and J. Wang, *J. Nanosci. Nanotechnol.* 11, 9464 (**2011**).
7. M. Samal, J. M. Lee, W. I. Park, D. K. Yi, U. Paik, and C.-L. Lee, *J. Nanosci. Nanotechnol.* 11, 10069 (**2011**).
8. J. K. Wassei and R. B. Kaner, *Mater. Today* 13, 52 (**2010**).
9. X. Li, W. Cai, J. An, S. Kim, J. Nah, D. Yang, R. Piner, A. Velamakanni, I. Jung, E. Tutuc, S. K. Banerjee, L. Colombo, and R. S. Ruoff, *Science* 324, 1312 (**2009**).
10. J. H. Rho, S. H. Jang, Y. D. Ko, S. J. Kang, D. W. Kim, J. S. Chung, M. Y. Kim, M. S. Han, and E. J. Choi, *Appl. Phys. Lett.* 95, 241906 (**2009**).
11. A. B. Kuzmenko, E. van Heumen, F. Carbone, and D. van der Marel, *Phys. Rev. Lett.* 100, 117401 (**2008**).

12. K. S. Novoselov, A. K. Geim, S. V. Morozov, D. Jiang, Y. Zhang, S. V. Dubonos, I. V. Grigorieva, and A. A. Firsov, *Science* 306, 666 **(2004)**.
13. V. Perebeinos and P. Avouris, *Phys. Rev. B* 81, 195442 **(2010)**.
14. A. Konar, T. Fang, and D. Jena, *Phys. Rev. B* 82, 115452 **(2010)**.
15. L. A. Ponomarenko, R. yang, T. M. Mohiuddin, M. I. Katsnelson, K. S. Novoselov, S. V. Morozov, A. A. Zhkov, F. Schedin, E. W. Hill, and A. K. Geim, *Phys. Rev. Lett.* 102, 206603 **(2009)**.
16. K. S. Kim, Y. Zhao, H. Jang, S. Y. Lee, J. M. Kim, K. S. Kim, J.-H. Ahn, P. Kim, J.-Y. Choi, and B. H. Hong, *Nature* (London) 457, 706 **(2009)**.

Received: 1 August 2011. Accepted: 19 January 2012.

RESEARCH ARTICLE